High-order mesh optimization techniques for compressible shock hydrodynamic applications

WCCM ECCOMAS Congress 2021, Paris, France

11-15 January 2021

CASC
Center for Applied Scientific Computing

Ketan Mittal
V. Dobrev, P. Knupp, Tz. Kolev, and V. Tomov

LLNL-PRES-XXXXXX
This work was performed under the auspices of the U.S. Department of Energy by Lawrence Livermore National Laboratory under contract DE-AC52-07NA27344. Lawrence Livermore National Security, LLC

Lawrence Livermore National Laboratory

Overview

- Introduction
- Target Matrix Optimization Paradigm (TMOP) for mesh optimization
  - r-adaptivity
- hr-adaptivity
- Applications
- Future work

Introduction

- We are interested in optimizing meshes for multi-material ALE Hydrodynamics [1]. For N materials and a material index $k = 1 \ldots N$, the system of interest is:

$$\frac{\mathrm{d}\eta_k}{\mathrm{d}t} = \alpha_k \tag{1}$$

$$\frac{\mathrm{d}(\eta_k \rho_k)}{\mathrm{d}t} = -\eta_k \rho_k \nabla \cdot u \tag{2}$$

$$\rho_k \frac{\mathrm{d}u}{\mathrm{d}t} = \nabla \cdot \sum_k \eta_k \sigma_k \tag{3}$$

$$\eta_k \rho_k \frac{\mathrm{d}e_k}{\mathrm{d}t} = \eta_k \sigma_k \cdot \nabla u - \bar{p}\alpha_k \tag{4}$$

Introduction

- Why mesh optimization?

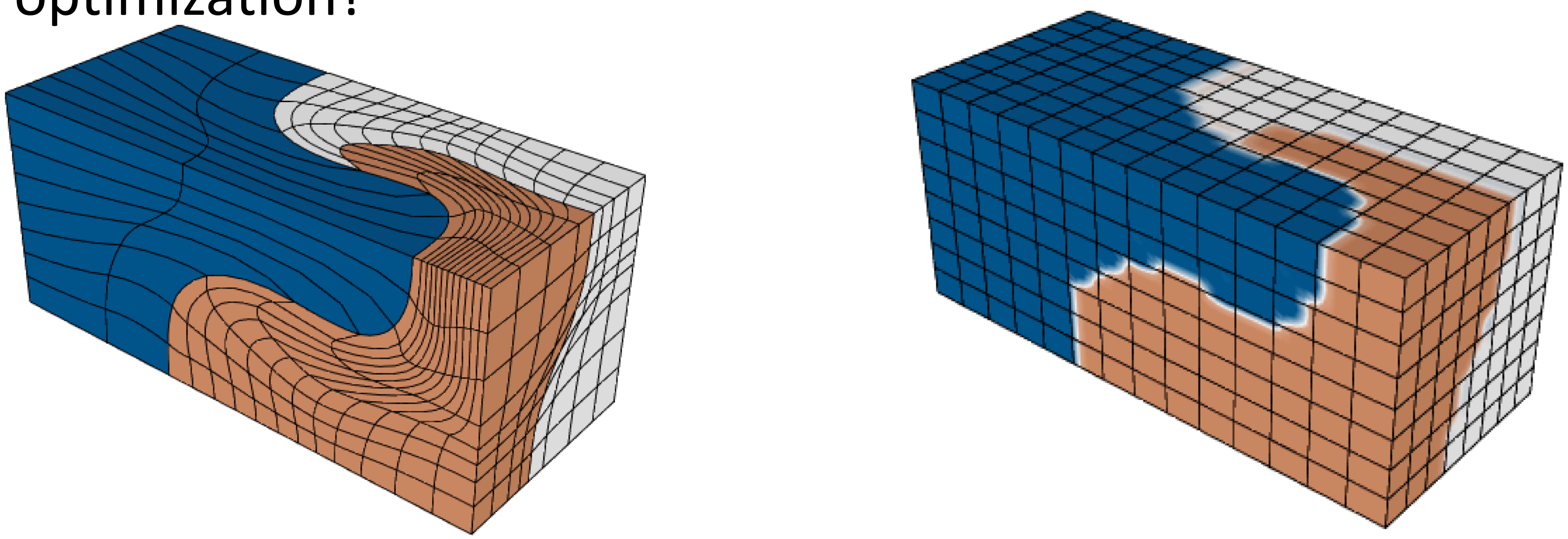

3D triple point problem on a static mesh and on a moving mesh with Lagrangian framework.

- Lagrangian meshes can get large deformations which lead to small time step size or even tangling of the finite elements.
- Static meshes can lead to numerical dissipation as materials evolve in time.
- Mesh optimization can help reduce numerical dissipation and prevent mesh tangling.
  - Also improve computational efficiency of the calculation (#dofs for a given accuracy).

Target Matrix Optimization Paradigm (TMOP)

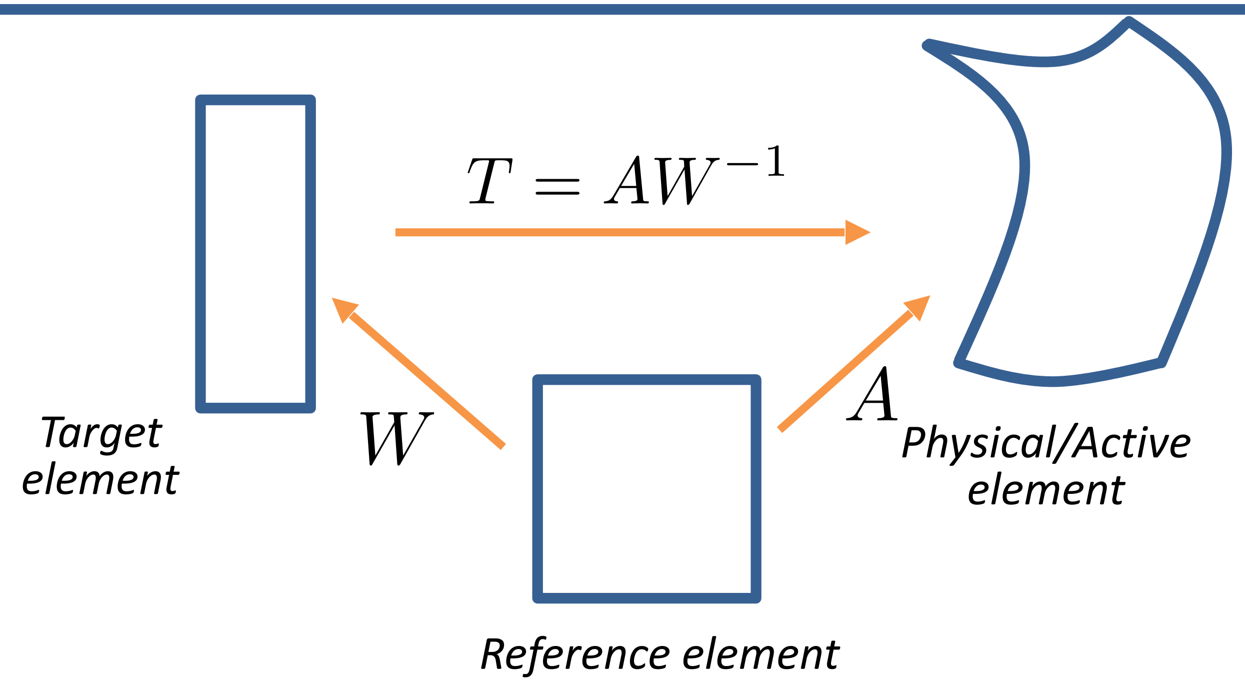

- Any Jacobian transformation can be represented using four geometric parameters:

$$W = \underbrace{\zeta}_{\text{[volume]}} \; \underbrace{R}_{\text{[rotation]}} \; \underbrace{Q}_{\text{[skewness]}} \; \underbrace{D}_{\text{[aspect-ratio]}}$$

- The transformation T from the active to target element can be defined using the Jacobian transformation A and W.

TMOP Mesh Quality Metrics

- Quality metric $\mu(T)$ is a measure of the deviation between the active and target Jacobian transformation.

- Different metrics depend on different geometric parameters.

  - $\texttt{Shape}$ metric - depends on Skew (Q) and Aspect-ratio (D). $\mu_2(T) = 0.5\frac{|T|^2}{\det(T)} - 1$

  - $\texttt{Size}$ metric - depends on ζ. $\mu_{77}(T) = 0.5\left(\det(T) - \frac{1}{\det(T)}\right)^2$

  - Other kinds include $\texttt{Alignment}$, $\texttt{Shape} + \texttt{Size}$, $\texttt{Shape} + \texttt{Alignment}$, etc.

    Over 100 different metrics divided into 8 metric types.

  - We typically deploy metrics that control shape and size of the elements, but seldom also use metrics for mesh alignment.

r-adaptivity with TMOP

- Using the quality metric and the Jacobian transformation T, the TMOP objective function is defined as:

$$F(\mathbf{x}) = \sum_{E\in\mathcal{M}} F_E(\mathbf{x}_E) = \sum_{E(\mathbf{x}_E)} \int_{E_t} \omega(\mathbf{x})\mu(T(\mathbf{x}))d\mathbf{x}_t$$

where $\mathbf{x}$ represents mesh coordinates, ω is a user-defined spatial weight. The element-by-element integral is computed as:

$$\sum_{E\in\mathcal{M}} \int_{E_t} \omega(\mathbf{x}_t)\mu(T(\mathbf{x}_t))d\mathbf{x}_t = \frac{1}{N_E}\sum_{E\in\mathcal{M}} \sum_{\mathbf{x}_q\in E_t} w_q \det(W(\bar{\mathbf{x}}_q))\,\omega(\mathbf{x}_q)\mu(T(\mathbf{x}_q))$$

- In practice, we can use multiple metrics with different spatial weights.
- r-adaptivity - $F(\mathbf{x})$ is minimized using a technique such as the Newton's method to optimize the mesh [2].

Target Construction

- Use of TMOP relies on choice of W and a compatible quality metric.
- W is defined using any combination of the four geometric parameters based on the mesh optimization goal. [3]
- For practical implementations, W is derived from discrete simulation data at run-time.
- Consider a simple 2D example where the material interface is not aligned with the mesh:

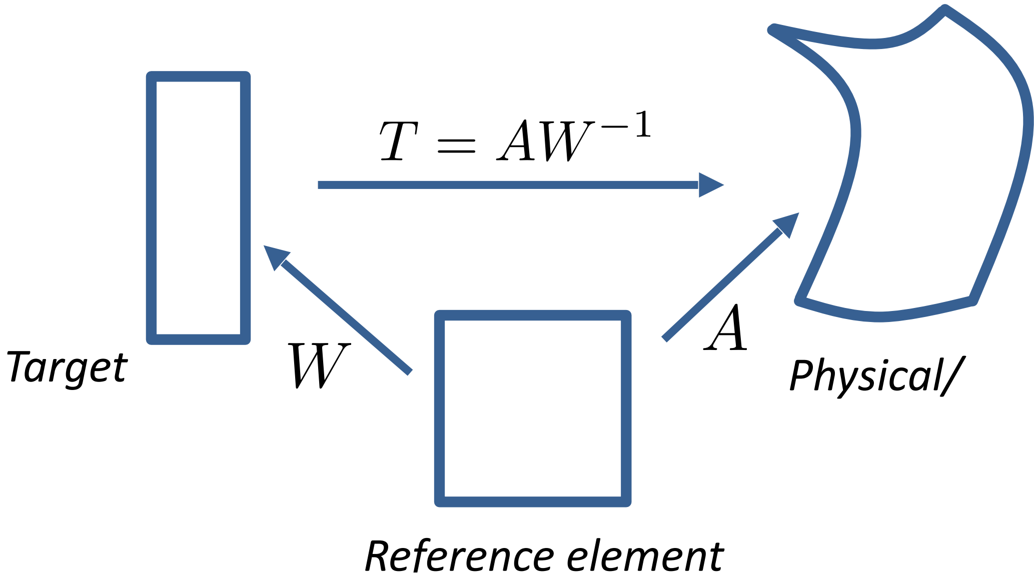

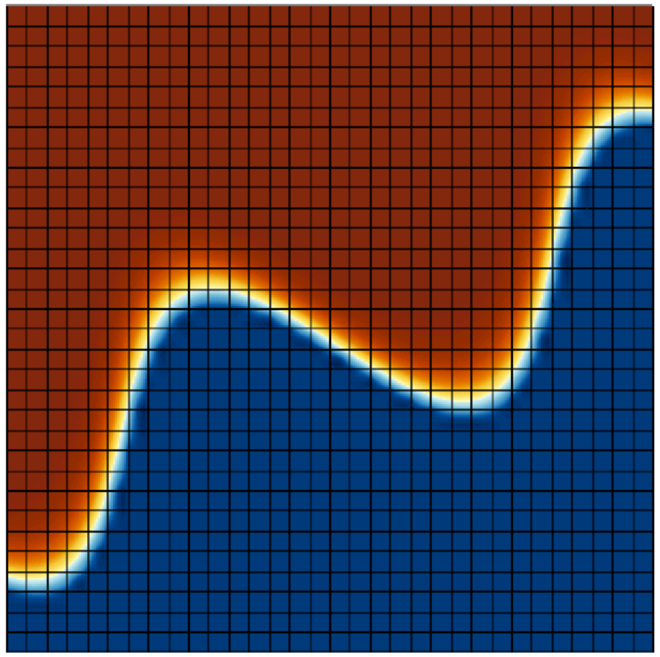

Simulation data - material indicator (η)

Target Construction

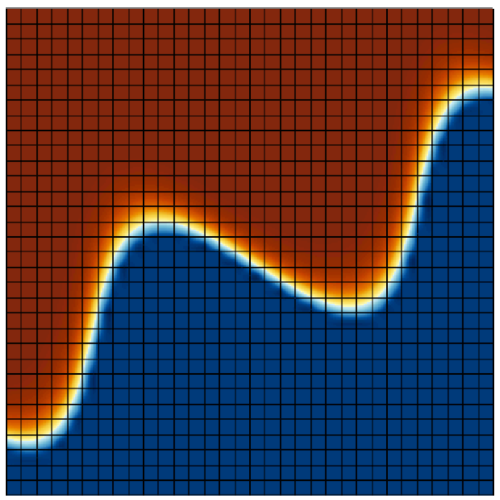

Simulation data
material indicator (η)

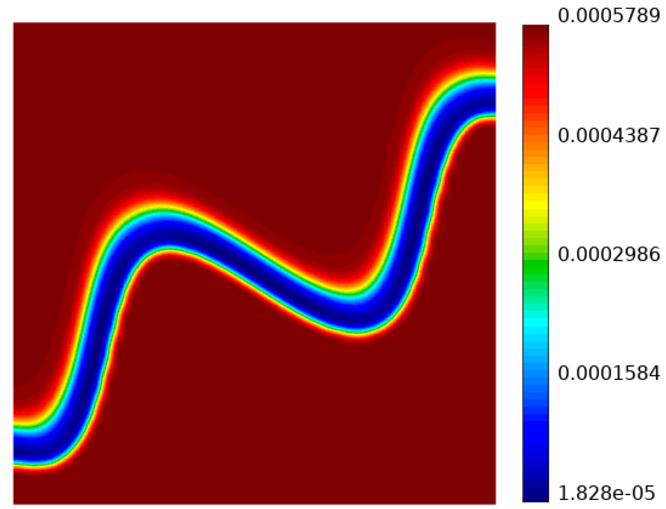

Size - $\zeta \propto 1/|\nabla \eta|$

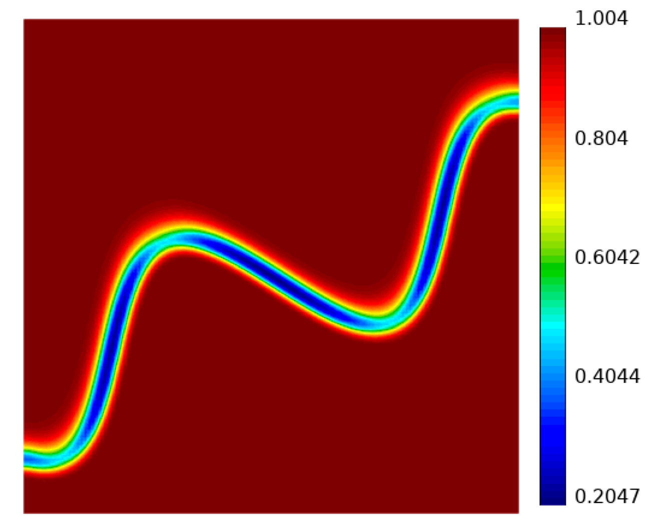

Aspect-Ratio - $\rho \propto |\eta_x/\eta_y|$

- $$W = \sqrt{\zeta} \begin{bmatrix} 1 & 0 \\ 0 & 1 \end{bmatrix} \begin{bmatrix} 1 & \cos\phi \\ 0 & \sin\phi \end{bmatrix} \begin{bmatrix} \frac{1}{\sqrt{\rho}} & 0 \\ 0 & \sqrt{\rho} \end{bmatrix},$$
- $\phi = \frac{\pi}{2}$ for an ideal square.
- Use a $\texttt{Shape} + \texttt{Size}$ metric, $\mu_7 = |T - T^{-t}|^2$

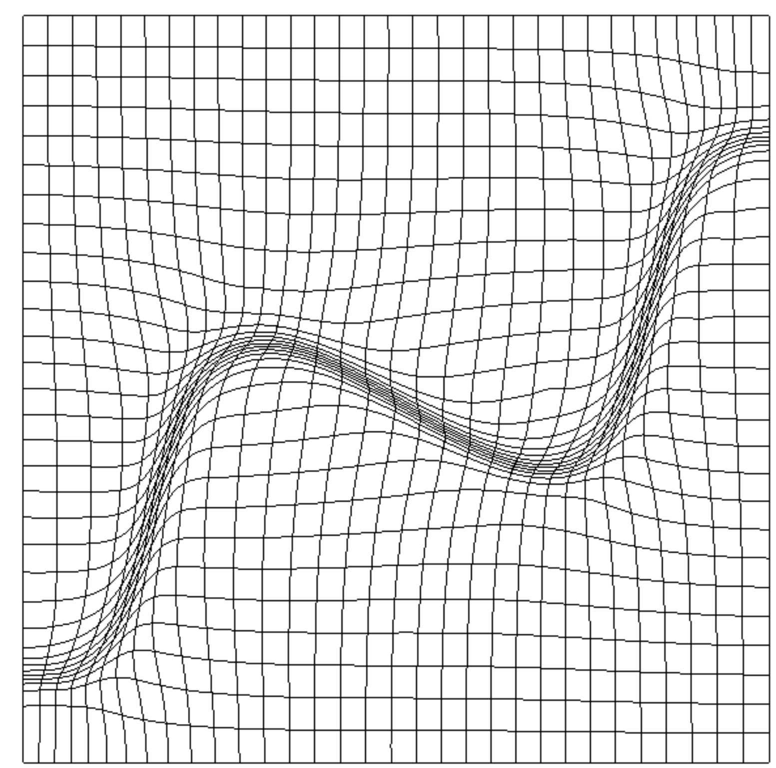

Discrete Function Transfer During and After Mesh Optimization

- During and after mesh-optimization, the discrete functions must be mapped from the original mesh to the moved mesh.
  - Interpolation using FindPoints [4], $\mathbf{x_s} \in \Omega_s \rightarrow e, \mathbf{r} \in \Omega_0$
  - PDE-based remap [5], $\tau \in [0,1]$, $\mathbf{u} = \mathbf{x_s} - \mathbf{x_0}$

$$\frac{\partial \eta}{\partial \tau} = \mathbf{u} \cdot \nabla \eta, \qquad \eta(\mathbf{x_0}, 0) = \eta_0(\mathbf{x_0})$$

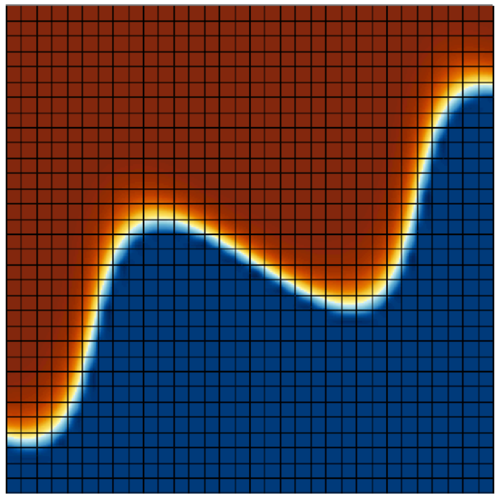

$\eta_0(\mathbf{x_0})$

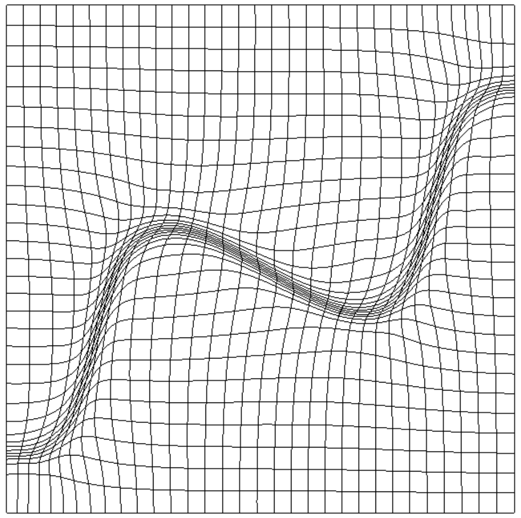

$\mathbf{x_s}$

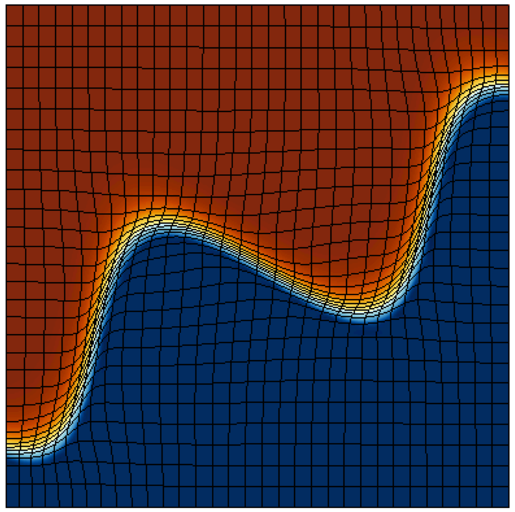

$\eta(\mathbf{x_s})$

h-adaptivity

- Effectiveness of r-adaptivity can be limited due to the topology of the original mesh.
- h-adaptivity introduces addition degrees of freedom by splitting existing elements.
- Nonconforming high-order mesh refinement framework introduced by Cerveny et al. [6]
  - Supports **nonconforming isotropic** and **anisotropic** refinement/derefinement in 2D and 3D for **triangles/quads** and **tetrahedrons/cubes**.
  - Requires use of an error estimor for refinement/derefinement decisions during simulation.

AMR for Mesh Optimization

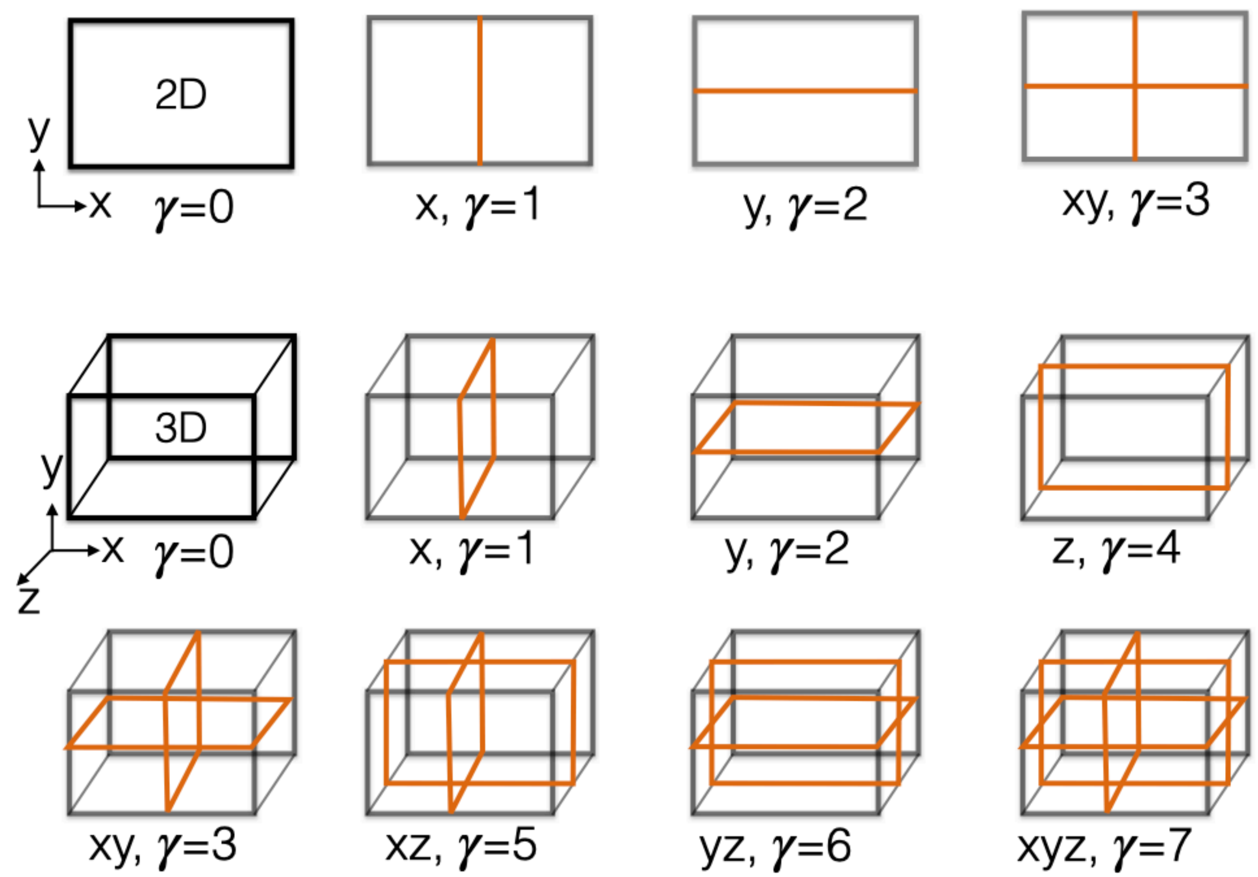

Different types of refinements for a quad and a cube

- Anisotropic refinements impact the shape and size of an element, and isotropic refinement impacts only the size of an element.

- Refinements also impact skew, but this impact cannot be directly controlled.

TMOP-based Refinement Error Estimator

- Based on μ, define Γ as the set of refinement types to be considered:
  - $\texttt{Shape}$ metric - $\gamma = 1{,}2$ in 2D and 1-6 in 3D.
  - $\texttt{Size}$ metric - $\gamma = 3$ in 2D and 7 in 3D.
  - $\texttt{Shape} + \texttt{Size}$ metric - $\gamma = 1 - 3$ in 2D and 1-7 in 3D.
- For a given element E and refinement type γ:

Difference in energy for a given refinement. → $$\Delta F_E^\gamma = F_E^{\gamma=0} - \frac{F_E^\gamma}{N_c},$$

Sum of TMOP energy for children of a given element. → where $F_E^\gamma = \sum_{i=1}^{N_c} F_{E_c}$

TMOP energy for a given element. → $$F_E = \sum_{\mathbf{x}_q \in E_t} w_q \det(W(\bar{\mathbf{x}}_q))\, \omega(\mathbf{x}_q) \mu(T(\mathbf{x}_q))$$

- Refinement type is picked based on: $\max_\gamma \Delta F_E^\gamma, \;\; \gamma \in \Gamma$

TMOP-based Refinement Error Estimator

- In practice, determining F_E^γ requires the element E being considered to be refined and all discrete functions must be mapped to its children E_c.
    - Trivial via finite element interpolation matrices that can be robustly constructed for a given γ.

TMOP-based Derefinement Error Estimator

- Derefinement is important for time-dependent problems where regions that require resolution can change with time.
- Elements that are already refined, are considered for derefinement:
  - If E_p is an element that was refined to span N_c children at a previous iteration:

Difference in energy for a derefinement.

$$\Delta F_{E_p} = \sum_{i=1}^{N_c} \frac{F_{E_c}}{N_c} - F_{E_p}$$

- ΔF_E^γ for refinement and ΔF_{E_p} for derefinement are compliments of each other.

hr-adaptivity

$\mathbf{x}_0$ - original mesh
μ - TMOP quality metric
ϵ - Newton convergence
N_h - h-adaptivity iterations per step.

Target construction

N_R - Number of elements refined at previous iteration metric
N_D - Number of elements derefined at previous iteration

r-adaptivity with Newton's method (ϵ)

N_h iterations of h-adaptivity

Algorithm 1: $hr-$adaptivity

Input: $\mathbf{x}_0$, μ, ε, N_h.

Output: $\mathbf{x}_s$ (initialized to $\mathbf{x}_0$).

Construct W_i for each integration-point i using target-construction. [25]

while $N_R \neq 0$ or $N_D \neq 0$ **do**

  $r-$adaptivity:

  $\mathbf{x}_s \to \arg\min_{\mathbf{x}} \sum_{E\in\mathscr{M}} \sum_{\mathbf{x}_q \in E_t} w_q \det(W(\bar{\mathbf{x}}_q))\, \omega(\mathbf{x}_q)\mu(T(\mathbf{x}_q))$. [1]

  $h-$adaptivity:

  for $i \in 1 \dots N_h$ **do**

    $\forall\ E_p \in \mathscr{M}$, determine ΔF_{E_p}. (10) [Derefinement estimator]

    Derefine element E_p if $\Delta F_{E_p} > 0$.

    $\forall\ E \in \mathscr{M}$, determine $\Delta F_E^\gamma\ \forall\ \gamma \in \Gamma$. (7) [Refinement estimator]

    Refine element E based on $\max_\gamma \Delta F_E^\gamma$. [13]

  end

end

- Note: quality metric can be different for r- and h-adaptivity component.

Application I - 2D Benchmark Using Poisson Equation

- Solve the Poisson problem:

$$\nabla^2 u = f, \qquad \Omega = [0,1]^2$$

with a known exact solution to mimic a sharp circular wave front of radius r centered at (x_c, y_c)

$$u = \arctan\left[\alpha\left(\sqrt{(x-x_c)^2 + (y-y_c)^2} - r\right)\right]$$

- $\alpha = 200,\ (x_c, y_c) = (-0.05, -0.05),\ r = 0.7$

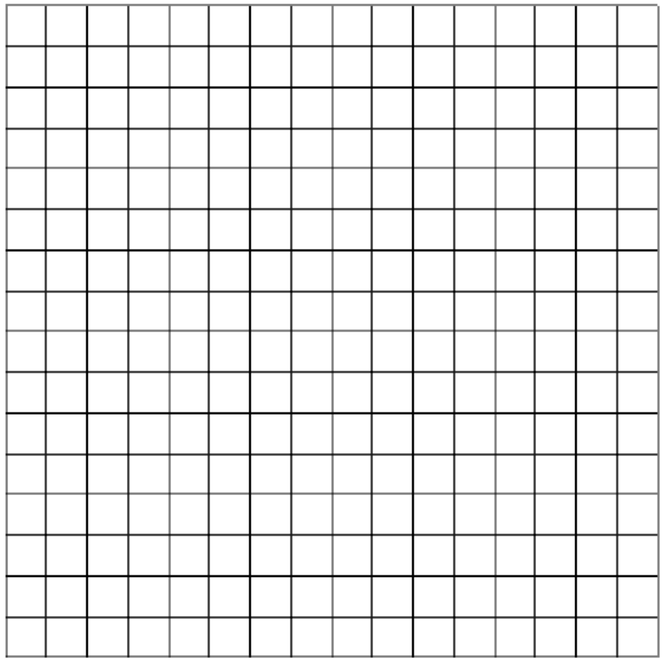

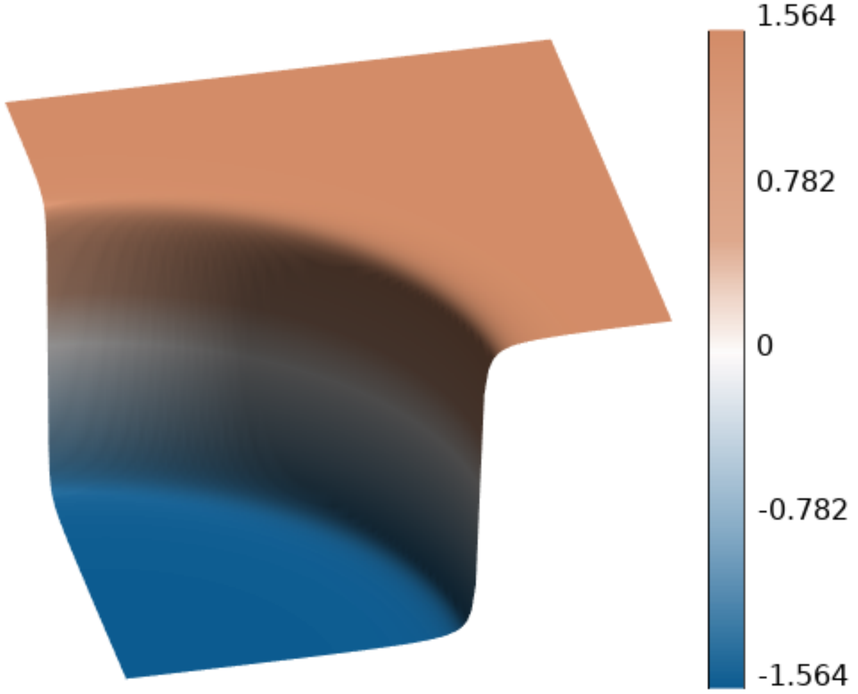

Application I - 2D Benchmark Using Poisson Equation

- Target construction using gradient of the discrete function on the mesh, as earlier.

$$W = \sqrt{\zeta}\begin{bmatrix}1 & 0\\ 0 & 1\end{bmatrix}\begin{bmatrix}1 & \cos\phi\\ 0 & \sin\phi\end{bmatrix}\begin{bmatrix}\frac{1}{\sqrt{\rho}} & 0\\ 0 & \sqrt{\rho}\end{bmatrix}$$

- To compare *h*-, *r*-, and *hr*-adaptivity, we start with a mesh and do 1 iteration of *h*- and/or *r*-adaptivity, using a $\mathtt{Shape} + \mathtt{Size}$ metric

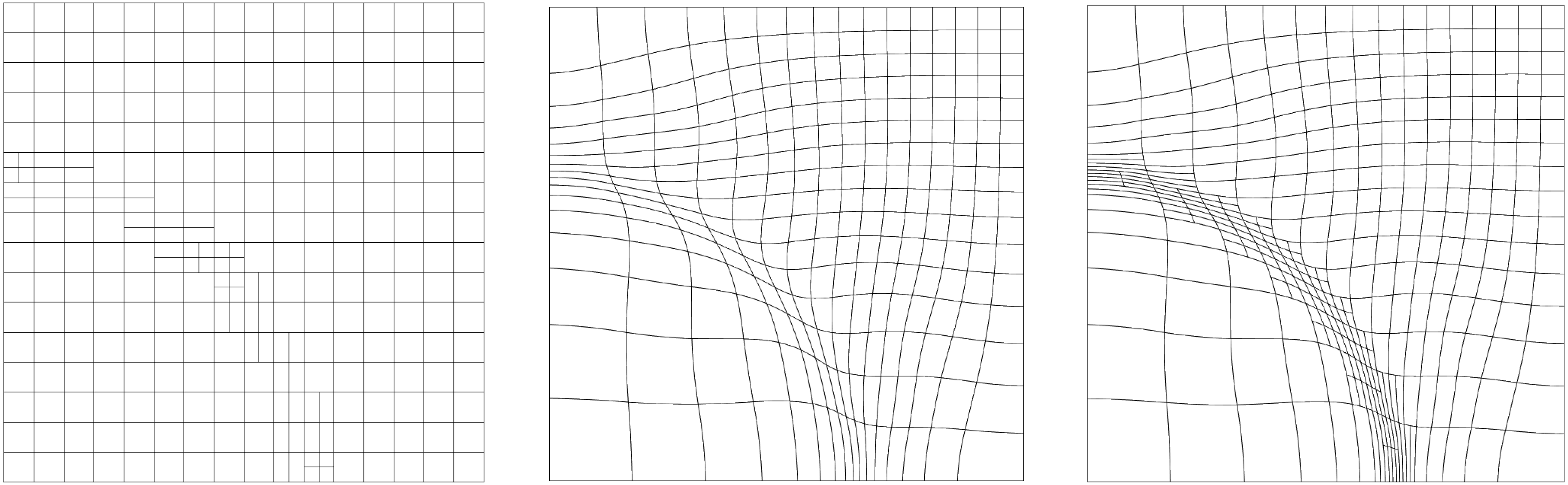

h-adaptivity r-adaptivity hr-adaptivity

Application I - 2D Benchmark Using Poisson Equation

- Error comparison for different adaptivity techniques shows effectiveness of *hr*-adaptivity.
- *hr*-adaptivity requires 66% fewer degrees of freedoms in comparison to *r*-adaptivity for a given accuracy in the solution.

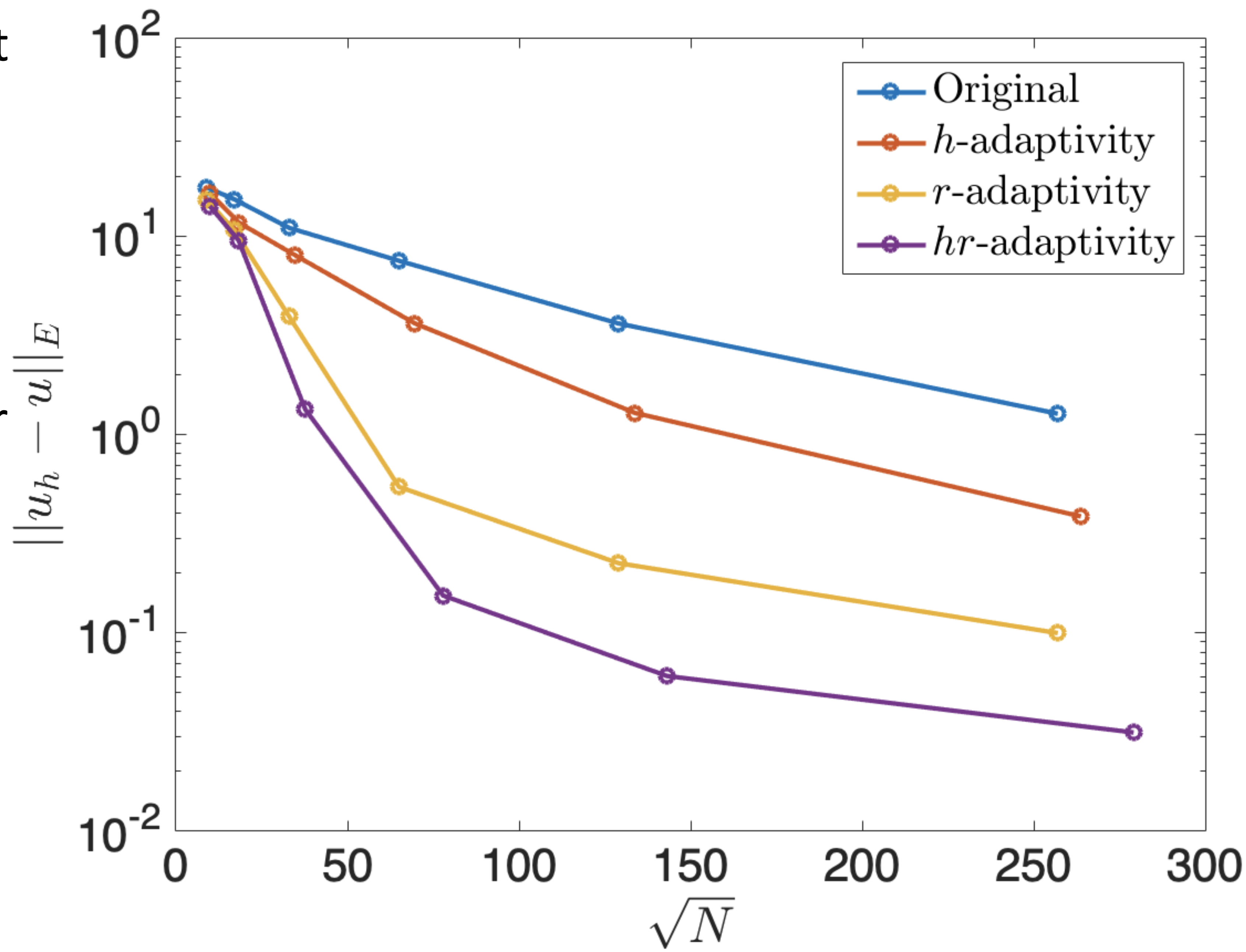

Application II - Analytic adaptivity

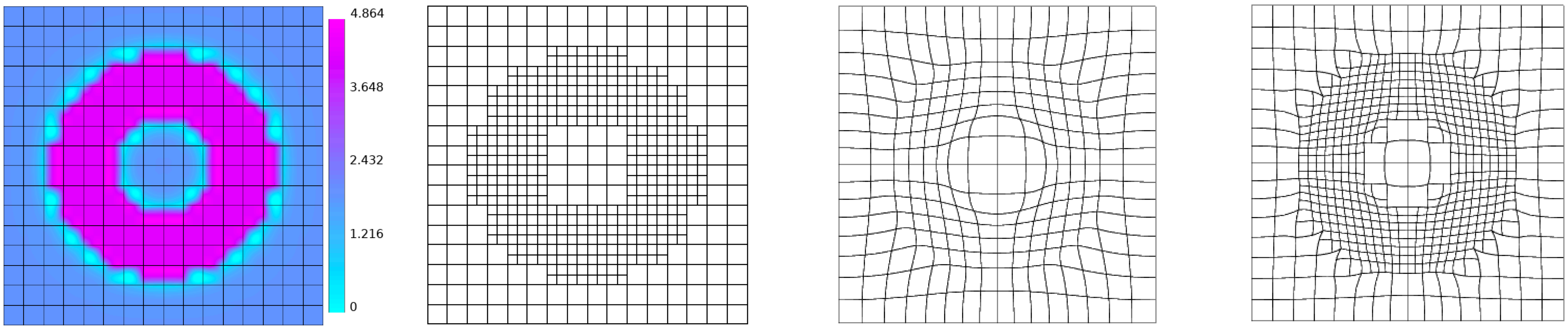

$N_E = 256$ | $N_E = 544, \Delta F = 21.9\,\%$ | $N_E = 256, \Delta F = 51.8\,\%$ | $N_E = 616, \Delta F = 67.3\,\%$

(a) μ_7^r (Shape + Size metric), μ_{55}^h (Size metric)

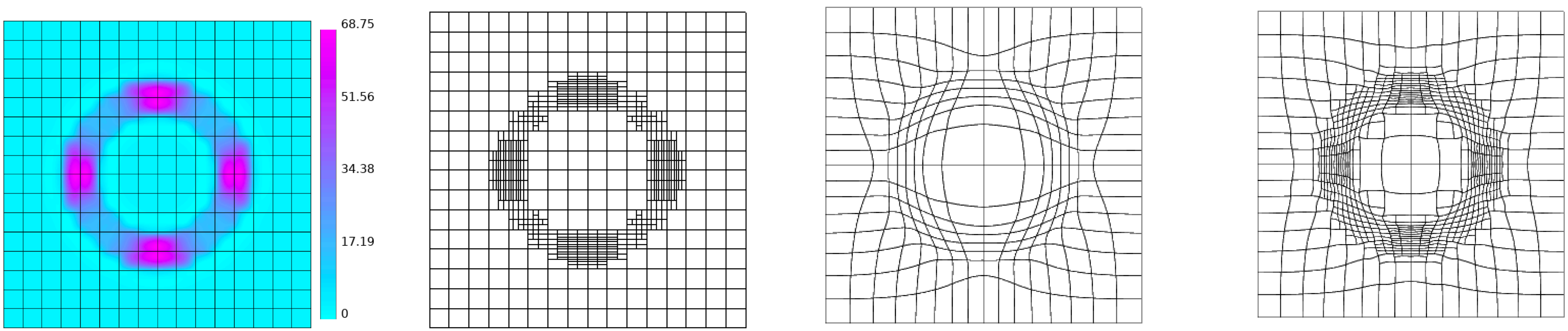

$N_E = 256$ | $N_E = 600, \Delta F = 65.6\,\%$ | $N_E = 256, \Delta F = 60.6\,\%$ | $N_E = 716, \Delta F = 85.3\,\%$

(b) μ_7 (Shape + Size metric)

Application II - Analytic adaptivity

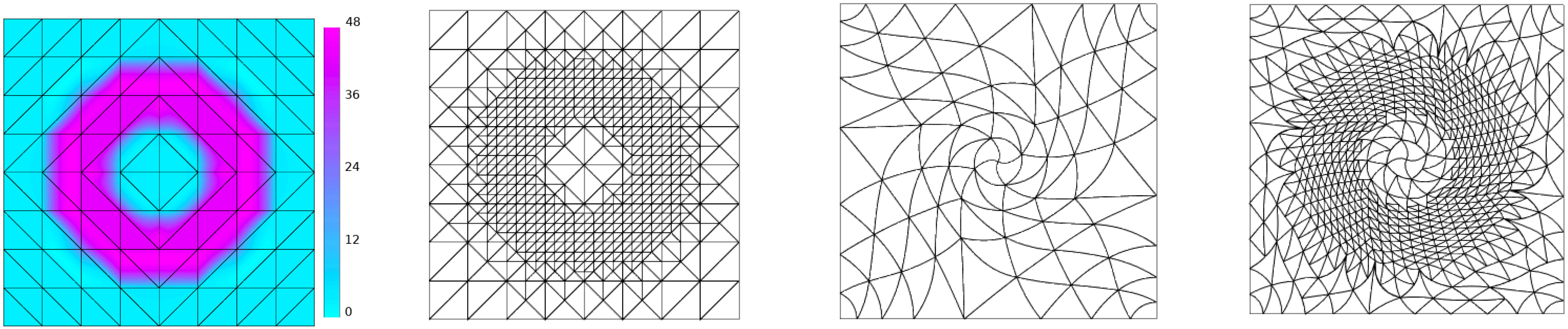

$N_E = 128$ | $N_E = 928, \Delta F = 62.4\,\%$ | $N_E = 128, \Delta F = 43.9\,\%$ | $N_E = 1100, \Delta F = 85.2\,\%$

(c) μ_7^r (Shape + Size metric), μ_{55}^h (Size metric)

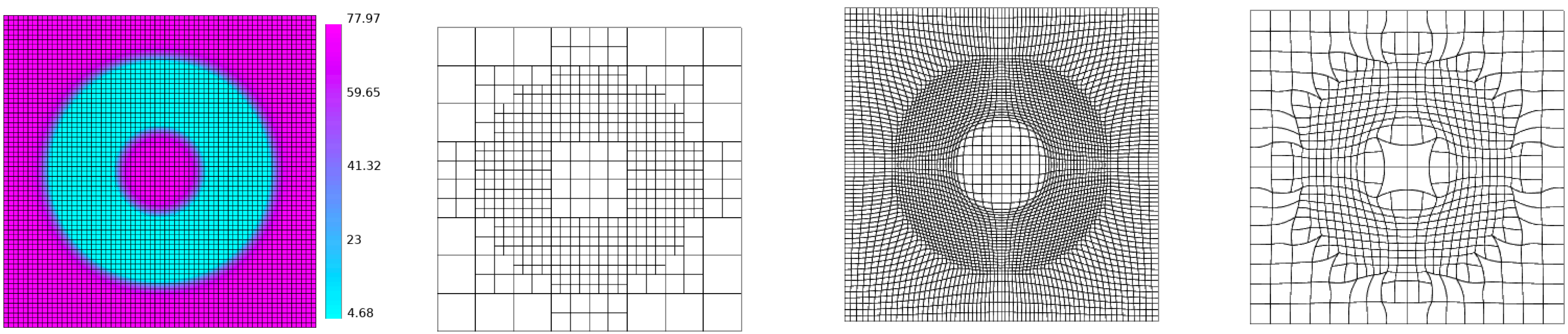

$N_E = 4096$ | $N_E = 484, \Delta F = 98.3\,\%$ | $N_E = 4096, \Delta F = 55.4\,\%$ | $N_E = 664, \Delta F = 98.6\,\%$

(d) μ_7^r (Shape + Size metric), μ_{55}^h (Size metric)

Application III - ALE Hydrodynamics 2D gas impactor

- High-velocity impact of gasses [7] using the Laghos [8] in MFEM.
- Large mesh deformations lead to mesh tangling in Lagrangian framework.
- TMOP-based *r*- and *hr*-adaptivity improves mesh quality and provides resolution in regions with material interaction:
  - $\mathtt{Shape} + \mathtt{Size}$ metric for *r*- and $\mathtt{Shape}$ metric for *h*-adaptivity component.
  - Material indicator used for target construction.

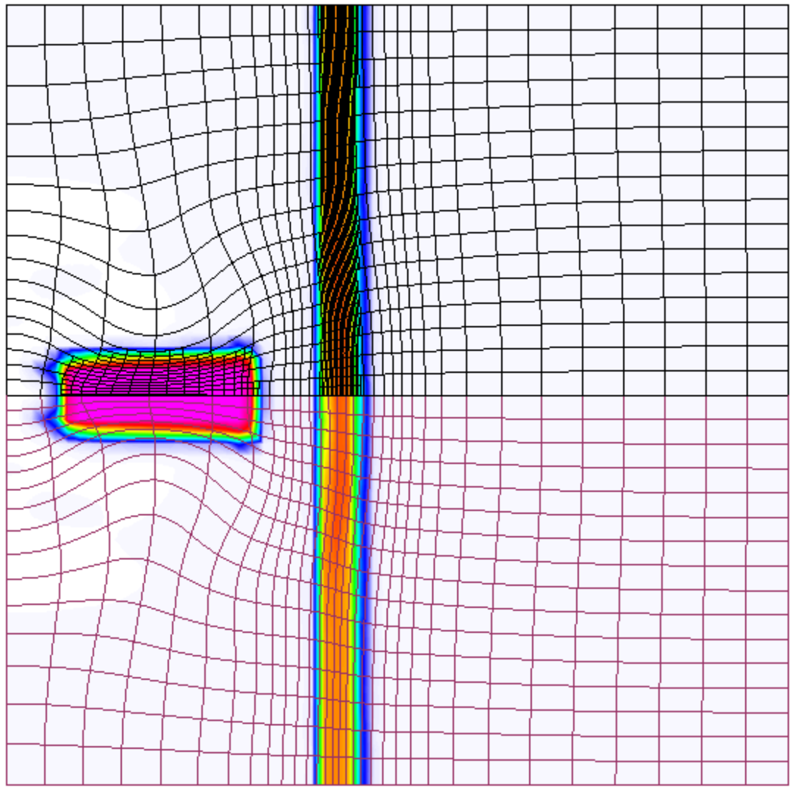
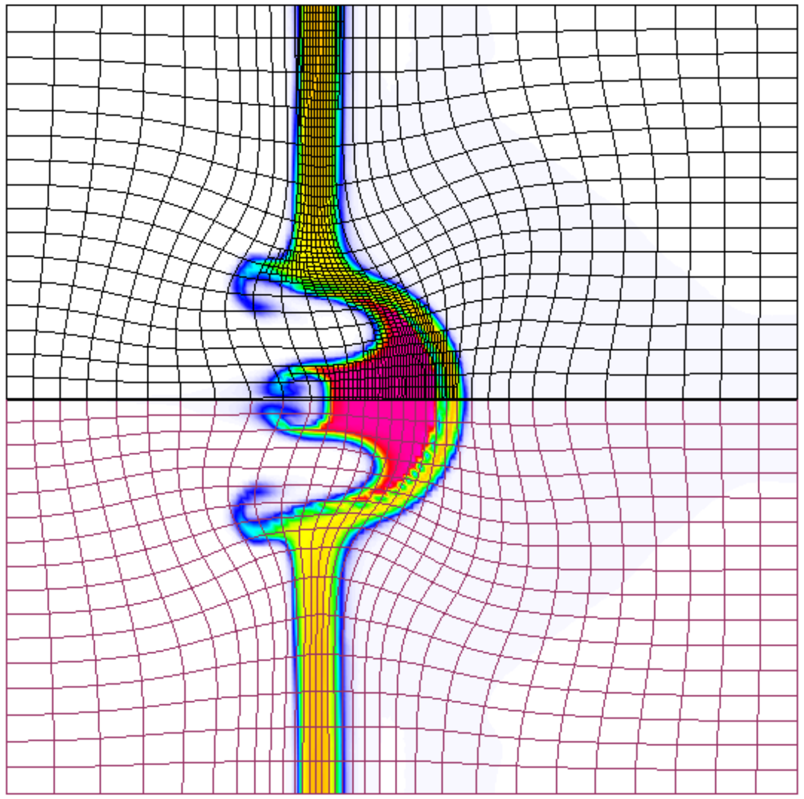
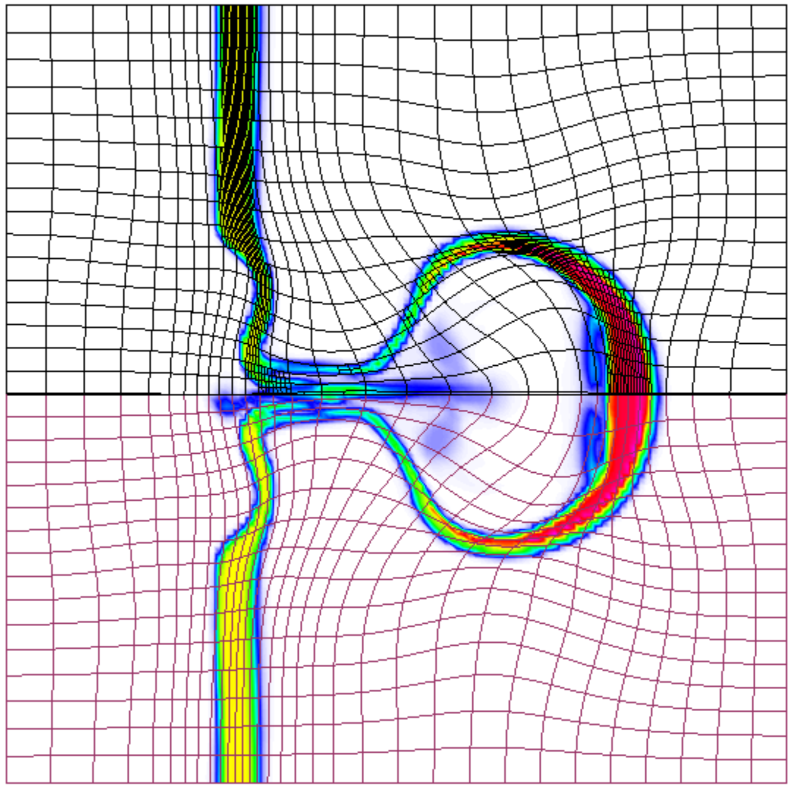

Application IV - ALE Hydrodynamics 3D Triple Point

- 3D triple point problem [9].
- $\texttt{Shape} + \texttt{Size}$ metric for *r*- and $\texttt{Size}$ metric for *h*-adaptivity component.
- To quantify the comparison between these meshes, we look at how well the original material indicator can be represented on each of the meshes in comparison to the mesh from Lagrangian framework.

$$e = \int_{\Omega} \left(\eta_L(\mathbf{x}_L) - \eta(\mathbf{x}_s) \right)^2$$

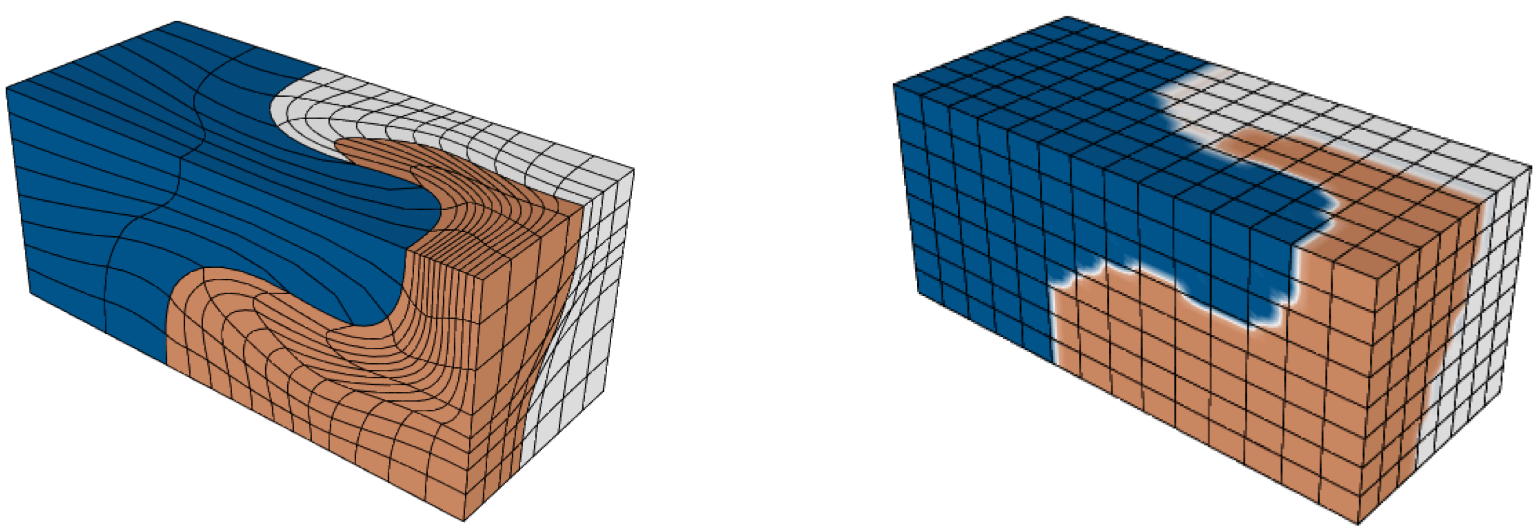

(a) Lagrangian mesh (b) Original mesh

$\eta_L(\mathbf{x}_L)$

Application IV - ALE Hydrodynamics 3D Triple Point

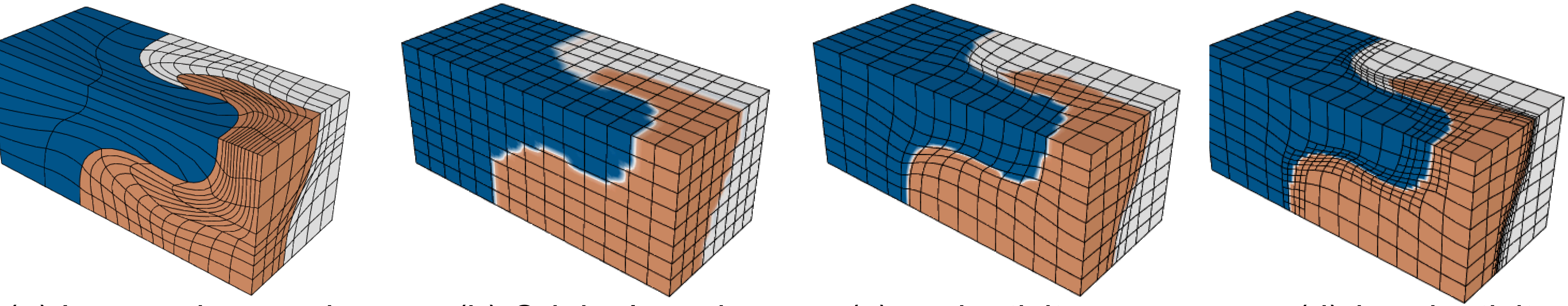

(a) Lagrangian mesh $\eta_L(\mathbf{x}_L)$

(b) Original mesh $e = 1.71$

(c) *r*-adaptivity $e = 0.62$

(d) *hr*-adaptivity $e = 0.078$

- Volumetric error is almost an order of magnitude lower for the *hr*−adaptivity mesh in comparison to *r*−adaptivity and about 20x lower in comparison to the uniform hexahedron mesh.

Conclusion & Future Work

- TMOP-based mesh optimization enables *hr*-adaptivity for nonconforming high-order meshes.
- Novel element-by-element TMOP-based energy estimator determine elements and corresponding refinement type for *h*-adaptivity.
- Physics-dependent mesh optimization can significantly improve the computational performance of a mesh by reducing the number of degrees of freedom required for a given accuracy in the solution.
- Future work:
  - Integrate *hr*-adaptivity framework in the Laghos miniapp for optimization at runtime.
  - Explore integration of *p*-adaptivity in *hr*-adaptivity framework.

MFEM open source implementation

- All presented methods are (or will be) available in MFEM.
- MFEM contains **various** 2D and 3D mesh quality metrics, and different **6** target construction methods.
- Modular framework allows additional metrics and target construction approaches to be robustly integrated.
- User interface provided by the ***mesh_optimizer*** and ***pmesh_optimizer*** miniapps.
  - Choice of target construction / quality metric / adaptivity fields / parameters.
  - Visualization through GLVis.

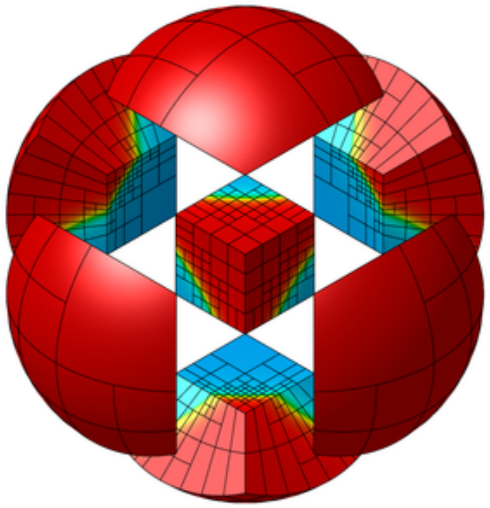

mfem.org

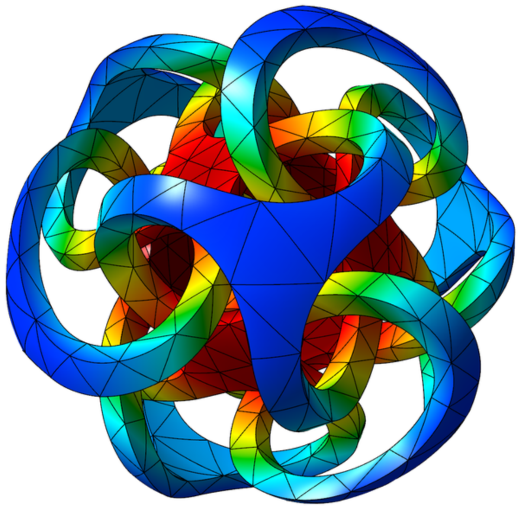

glvis.org

CASC

Center for Applied Scientific Computing

Lawrence Livermore National Laboratory

References

- [1] Anderson, Robert et al. “High-Order Multi-Material ALE Hydrodynamics”, *SIAM J. Sci. Comp.*(2018) 40(1):B32—B58.
- [2] Dobrev, Veselin, et al. "The target-matrix optimization paradigm for high-order meshes" *SIAM Journal on Scientific Computing* 41.1 (2019): B50-B68.
- [3] Knupp, P. *Target formulation and construction in mesh quality improvement*. No. LLNL-TR-795097. Lawrence Livermore National Lab.(LLNL), Livermore, CA (United States), 2019.
- [4] Mittal, Ketan et al. "Nonconforming Schwarz-spectral element methods for incompressible flow." *Computers & Fluids* 191 (2019): 104237.
- [5] Dobrev, Veselin, et al. "Towards simulation-driven optimization of high-order meshes by the Target-Matrix Optimization Paradigm." *International Meshing Roundtable*. Springer, Cham, 2018.
- [6] Cerveny, Jakub et al. “Nonconforming mesh refinement for high-order finite elements.”, *SIAM Journal on Scientific Computing* 41 (4) (2019) C367–C392.
- [7] Barlow, Andrew et al. “Constrained optimization framework for interface- aware sub-scale dynamics closure model for multimaterial cells in Lagrangian and arbitrary Lagrangian-Eulerian hydrodynamics.”, *Journal of Computational Physics.* 276 (2014) 92–135.
- [8] “Laghos: High-order Lagrangian hydrodynamics miniapp [Software]”, https://github. com/ceed/Laghos (2020)
- [9] Zeng, Xianyi et al. “A variational multiscale finite element method for monolithic ALE computations of shock hydrodynamics using nodal elements”, *Journal of Computational Physics* 315 (2016) 577–608.